Do Heavy and Light Users Differ in the Web-Page Viewing Patterns? Analysis of Their Eye-Tracking Records by Heat Maps and Networks of Transitions

Noriyuki Matsuda[1] and Haruhiko Takeuchi[2]

[1] Graduate School of Systems and Information Engineering, University of Tsukuba,
1-1-1 Tennou-dai, Tsukuba, Ibaraki 305-8573, Japan
mazda@sk.tsukuba.ac.jp

[2] National Institute of Advanced Industrial Science and Technology (AIST),
Central 6, 1-1-1 Higashi, Tsukuba, Ibaraki 305-8566, Japan
takeuchi.h@aist.go.jp

Abstract: **Web page viewing patterns were compared between heavy and light users with special foci on the cumulative importance (by the number of fixations and loops) and relative importance (by the network properties). To this end, the eye-tracking records obtained from 20 Ss who viewed 10 top web pages were coded into 5×5 segments imposed on the display. Networks were constructed from transitions of fixations among the segments. The relative importance was investigated on the individual nodes (core-peripheral) and the groups of nodes (by clique-based communities and the core neighborhoods). Joint analysis was conducted following the separate inspections on the cumulative and relative importance. Both similarities and dissimilarities between the user groups were reported with consideration to the nature of measurement.**

Keywords: heat map, loop, network analysis, core-peripheral nodes, clique, neighborhood.

I. Introduction

An eye-tracking record of a web page viewer contains rich information about the locations and shifts of his/her attention across a given page. It is generally held that one tends to gaze at the attractive contents than others, more frequently or longer (see [13] for the introductory information).

A heat map is a popular method to visualize the cumulative importance in the fixation records by coloring areas according to the heat as measured by the frequency of fixations on the areas of interest (AOI) (see [2][6][7][14]). A heat map augmented by scan paths (e.g., [13]) provides additional information, i.e., shifts of attention (see also [5] [9] for interesting approaches to the path presentation). However, it is hard to compare multiple maps in the absence of good algorithms for synthesizing the paths. Most serious shortcoming is the lack of a method for analyzing the dynamic importance in the transitions (see [10] [11]).

Matsuda et al. [10] demonstrated the plausibility of network analysis for identifying most and least important areas as well as densely connected areas set on the web pages. In the subsequent work [11], they attempted a joint analysis of static

(i.e., cumulative) and dynamic (i.e., relational) importance within the framework of network representation, by treating heat maps as unconnected networks. The correspondence between the two types of importance was fairly good.

Although their approach and the findings are very intriguing, they did not fully utilize the vital information in the data that seems to have special bearings on the web page viewing behavior, i.e., the distinction of heavy and light Internet users. Hence, we will compare in the present paper the two groups using the same data with some modifications in the treatment of dynamic importance to be explained shortly.

A. Network representation of eye-fixation records

Given areas of interest (AOI) set on a screen, a researcher can obtain a sequence of fixated areas for a given viewer. Multiple sequences result from repeated trails of a single or collective viewer(s). The present study will deal with the latter data.

The following two sequences suffice to illustrate the point, given a 3×3 AOI coded in upper case letters {A, B,..., I} (see also Appendix A of [11]).

Seq_1 = <ACCBFGGGAEBF>; length=12
Seq_2 = <BAABCBDEHD>; length=10

The successive codes such as CC and GGG in Seq_1 result from repeated (or sustained) fixations called loops in network analysis. The frequencies of the codes appearing in the sequences serve the basis of the heat map:

[A/4, B/5, C/3, D/2, E/2, F/2, G/3, H/1, I/0]

The segment 'I', with no fixation, will be treated as an isolated node in the network.

Anyone with some programming background can easily construct, from the sequences, a 9×9 adjacency matrix that records the number of transitions from code i to j. The matrix leads to a network that represents the codes as nodes and transitions as links. Figure 1 is the heat map overlaid with the network in the grid format. Obviously the merit of the joint display will increase, if the network is portrayed with the node and link properties to be explained next.
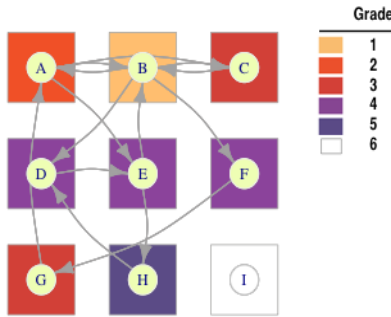
Figure 1. The heat map overlaid with the network

B. Network properties to be examined

Among various measures to characterize a network (see [12] [16]), we will focus on the basic properties about the linkage and those about individual nodes and groupings of nodes.

1) The link properties

A link from node i to j is one-way. If the connection is reciprocated from node j to i, the linkage is two-way, e.g., A↔B and B↔C shown in Figure 1. The *reciprocity* index measures the proportion of the number of two-way links in the total number of links. The other index of interest is the *transitivity* defined as the probability that the two nodes connected to a third node are also connected, e.g., the connections among <A, B, C>, <A, B, E> and <D, E, H> in Figure 1 are transitive.

2) Importance of Individual Nodes

 Nodes in a network differ in centrality which is measurable most notably by *degree, closeness* and *betweenness* ([16] [4]). In essence, a node is central in *degree* if it has the largest number of directly connected nodes; it is so in *closeness* if it is closest to the rest of the nodes in terms of geodesic distance; and, it is so in *betweenness* if it has the largest proportion of short-cut paths running among all pairs of nodes. According to [10] and [11], a node is the core of the network if it is central on all these indices that reflect different viewpoints. On the other hand, a node that is least central in all the indices is the peripheral one.

Basically, the three classical indices utilize the binary aspect of the links, whereas the ranking scores such as *PageRank* [1], and authority- and hub-(*AH*-) scores [8] incorporate the numerical weights of links. More precisely, the values of the elements of the adjacency matrix, say **A**, from which one can construct a network.

The two ranking methods are similar in both underlying ideas and mathematical solutions, but not identical as a matter of course. What they achieve is the rankings of nodes whose importance is recursively determined. In *PageRank*, the importance of a node increases as a function of the importance of nodes connected to it. In *AH*-scores, the authority and the hubness are mutually reinforcing. That is, the authority of a node increases as a function of the hubness of the nodes connecting to it, while the hubness of a node increases as a function of the authority of the nodes it is connected to.

PageRank derives the scores from the leading eigenvector of the transpose of a given adjacency matrix $\mathbf{A}^T$, after standardization by row. On the other hand, the authority- and the hub-scores are the values of the leading eigenvectors from $\mathbf{A}^T\mathbf{A}$ and $\mathbf{A}\mathbf{A}^T$, respectively.

In an effort to incorporate multiple perspectives, we will employ the aforementioned centrality indices and the ranking scores in determining the core-peripheral nodes. We assume that the importance of nodes is identifiable from the centralities and the rankings (see [10] [11]). The most and least important nodes will be referred to as the core(s) and peripheral(s), respectively.

3) The groupings of nodes

The two types groupings we will focus on are the core-neighborhood and the clique-based community. The former is a subgraph consisting of a core and the nodes directly connected to and/or from it. The latter is the union (∪) of the largest cliques in a network. The resulting grouping of nodes are congruent with the general notion of a community defined as a subgraph densely connected within relative to the external connections.

A clique is defined as a complete subgraph in which every pair of nodes is connected. For example, a subgraph <A, B, C> is a clique of size three, containing smaller cliques of size 2, i.e., <A, B>, <A, C>, and <B, C>. Were if nodes A and D connected, a subgraph <A, B, D, E> would be the largest clique of the network.   Instead of dealing with every clique, we will select the largest ones in a network to form the clique-based community by union.

In the previous studies of Matsuda et al. ([10][11]), the core-neighborhoods were sought within the corresponding communities, after making sure that the cores were included in the communities. By doing so, however, they might have truncated the core-neighborhoods. That is, the neighbors lying outside of the communities were not examined.   The non-overlapping part of the neighborhoods, i.e., Neighborhood – Community，were excluded before (see Figure 2). In the present work, the degree of overlap will be measured by the *Jaccard* index explained in Appendix.
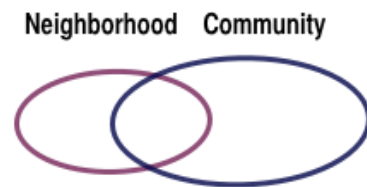

Figure 2. Venn's diagram for the two subgraphs

II. Method

(a) Subjects (Ss)

 Twenty residents (7 males and 13 females) living near a research institute AIST, Japan, participated in the experiment. They had normal or corrected vision, and their ages ranged from 19 to 48 years (30 on the average). Ten Ss were university students, five were housewives, and the rest were part-time job holders. They reported their level of Internet experiences on the basis of the number of hours they spend weekly in the net. Eleven were heavy users and nine were light users.

(b) Stimuli

The top pages of ten commercial web sites were selected from various business areas, including airline, e-commerce, finance and banking. The pages were classified into Types A, B and C depending on the layout of the principal part beneath the top layer (See Figure 3). The main area of Type A was sandwiched between subareas, while the main areas of Types B and C were accompanied by a single sub-area either on the left (B) or the right (C).
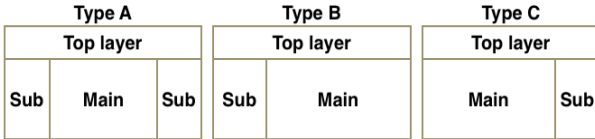

Type A			Type B		Type C	
Top layer			Top layer		Top layer	
Sub	Main	Sub	Sub	Main	Main	Sub

Figure 3. Layout types

(c) Apparatus and procedure

The stimuli were presented with 1024×768 pixel resolution on a TFT 17" display of a Tobii 1750 eye-tracking system at the rate of 50Hz. The web pages were randomly displayed to the *S*s one at a time, each time for a duration of 20 sec. The *S*s were asked to browse each page at their own pace. The English translation of the instructions is as follows: "Various Web pages will be shown on the computer display in turn. Please look at each page as you usually do until the screen darkens. Then, click the mouse button when you are ready to proceed." The *S*s were informed that the experiment would last for approximately five minutes.

(d) Segment coding and fixation sequences

A 5x5 mesh was imposed on the effective part of the screen stripped of white margins which had no text or graphics.

The segments were sequentially coded as shown in Figure 4 with a combination of the alphabetical and numerical labels for rows and columns, respectively: A1, A2, …, A5 for the first row; B1, …, B5 for the second; …; and, E1, …, E5 for the fifth.
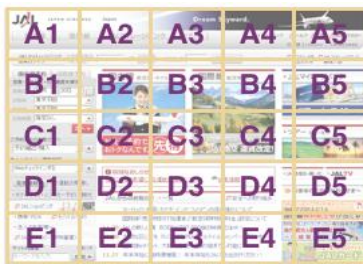

Figure 4. Segment coding

The raw tracking data of each subject, comprised of time-stamps and *xy*-coordinates, were transformed into the fixation points under the condition that *S*'s eyes stayed within a radius of 30 pixels for a 100-msec period. Then, each fixation record was translated into code sequences according to which segment fixation points fell in.

(e) Adjacency (transition) matrices

An adjacency matrix (25×25) was constructed for each page to record the frequencies of the fixation shifts from one segment to another aggregated across subjects from the fixation code sequences. The rows (and columns) of the matrix were arranged corresponding to the segment codes, as

follows:

[A1, A2, …, A5, B1, …, B5, …, E1, …, E5]

After separating the loops in the diagonal cells for heat analysis, the entries of the matrices were divided by the respective total frequencies. These standardized values were used as weights of links in computing the ranking indices.

(f) Heat maps

In order to color the segments by heat, the number of fixations (*NFix*) was classified first into six grades separated at the 25th, 50th, 75th, 95th and 100th percentiles (the 100th percentile is the maximum value.) The numeric code and the color assignment are shown in Table 1.

Table 1. Heat grade and color assignment

Grade	Color	Heat (*h*)
1		$h = 100p$
2		$95p \leq h < 100p$
3		$75p \leqq h < 95p$
4		$50p \leq h < 75p$
5		$25p \leq h < 50p$
6		$h < 25\ p$

Note. For instance, 50*p* denotes the 50th percentile value.

All the computations and graph layouts were carried out using the statistical package *R* [15] and its library package called *igraph* [3].

III. Results

The top 10 pages used as stimuli are abbreviated below as TP*n* hereinafter where *n* varies from 1 to 10. Among them, TP5 was eliminated owing to the broad white space. TP4 was also eliminated because the indices for the core identification did not agree well. The following eight pages were subjected to the analysis:

TP1, 3, 6 and 8 (Type A);
TP2 and 9 (Type B), and; TP7 and 10 (Type C)

Since the node names correspond to the segment codes, the terms *nodes* and *segments* would be used interchangeably in this section.

When appropriate, we will hereinafter add a prefix and a postfix to the TP notation like A_TP1H and A_TP1L in which A refers to the layout Type. The postfixes H and L denote the heavy and light users, respectively.

A. Examination of the two types of heat

The two types of heat of the segments are the number of fixations (*NFix*) and the number of loops (*NLop*). First, in the case of *NFix*, the Groups H and L were similar across pages in terms of the *Pearson*'s correlation coefficient (*r*) that ranged from .657 (A_TP1) to .932 (B_TP9), but not necessarily so in terms of the *Kendall*'s rank-order correlation coefficient (τ) that lied between .360 (A_TP1) to .828 (B_TP9) as shown in Table 2. The difference might be attributable to the sensitivity of the *Pearson*'s coefficient to extreme values.

Table 2. Pearson's and *Kendal*l's correlation coefficients
(*r* and τ) on *NFix* between groups

	Type A				Type B		Type C	
	TP1	TP3	TP6	TP8	TP2	TP9	TP7	TP10
r	.657	.729	.770	.843	.857	.932	.820	.918
t	.360	.556	.585	.660	.676	.828	.467	.801

Mean								
H	6.8	10.0	8.9	7.7	8.0	8.8	9.2	8.8
L	7.5	6.7	7.4	8.1	7.7	8.2	7.6	9.2
Median								
H	6.0	7.0	6.0	7.0	6.0	6.0	6.0	8.0
L	7.0	4.0	7.0	6.0	7.0	7.0	6.0	5.0

The group differences in the mean and the median *NFix* were dissimilar (see Table 3). While the mean of Group H was consistently greater than that of Group L across TPs by 1.8 (C_TP10) to 5.6 (A_TP3), the median of Group H was smaller than that of Group L on two TPs by 1.0 (A_TP6) and 4.0 (B_TP9). On the remaining TPs, the median of Group H was greater than that of Group L by 1.0 (C_TP7) to 7.0 (A_TP3). The mean is generally sensitive to extreme values, being a metric measure like the *Pearson*'s coefficient.

Table 3. Mean and median *NFix* by Group

	Type A				Type B		Type C	
	TP1	TP3	TP6	TP8	TP2	TP9	TP7	TP10
Mean								
H	23.0	22.7	22.0	22.6	23.0	24.0	22.9	23.6
L	19.6	17.1	19.6	19.8	19.8	20.6	18.7	21.8
Median								
H	22.0	22.0	14.0	23.0	22.0	19.0	18.0	22.0
L	17.0	15.0	18.0	18.0	20.0	20.0	17.0	18.0

Second, the user groups were similar across pages also in *NLop* as measured by *Pearson*'s coefficient, but the similarity was lower in *Kendall*'s (see Table 4). The coefficient *r* ranged from .663 (A_TP3) to .868 (B_TP9), whereas τ was consistently smaller than *r* on all pages, ranging from .495 (A_TP1) to .803 (B_TP9).

Table 4. *Pearson*'s and *Kendall*'s correlation coefficients (*r* and *t*) on *NLop* between groups

	Type A				Type B		Type C	
	TP1	TP3	TP6	TP8	TP2	TP9	TP7	TP10
r	.726	.663	.808	.807	.753	.868	.851	.856
τ	.495	.487	.420	.504	.570	.803	.508	.674

The group difference in mean *NLop* was not consistent (see Table 5). On five TPs, the mean of Group H was greater than that of Group L by 0.3 (B_TP2) to 3.3 (A_TP3). The opposite held for the remaining three TPs with the difference varying from 0.4 (A_TP8 and C_TP10).

Table 5. Mean and median *NLop* by Group

	Type A		TP6	TP8	Type B		Type C	
	TP1	TP3	TP6	TP8	TP2	TP9	TP7	TP10

The group difference in median *NLop* was not consistent, either, in the way dissimilar to the pattern of the mean. On only three TPs, the median of Group H was greater than that of Group L by 1.0 (A_TP8 and C_TP10) to 3.0 (A_TP3). On the remaining four TPs, the median of Group L was greater than that of Group H by 1.0 (A_TP1, Z_TP6, B_TP2, and B_TP9). There was no difference on C_TP7.

The two groups exhibited highly similar tendencies in the first two modal segments, i.e., two most heated segments, on the respective measures. As shown in Table 6, there were three identical pairs of the segments in *NFix* (A_TP6, B_TP2 and B_TP9) and four in *NLop* (A_TP6, BTP_9, C_TP7 and C_TP10), including ties. Among these, A_TP6 and B_TP9 were noteworthy, having identical pairs in both measures.

Mild agreement between the groups was found in the following patterns: pairs with the same primary segments (A_TP1 and C_TP10 on *NFix* and A_TP1 and B_TP2 on *NLop*), the reversed pairs (C_TP7 on *NFix* and A_TP3 A_TP8 in *NLop*), and, the primary segment in one pair but positioned second in the other pair (A_TP3, A_TP8, C_TP7 on *NFix*, and). There was no disagreement pattern.

Table 6. The first two modal segment pairs on *NFix* and *NLop* by Group

Index		A_TP1	A_TP3	A_TP6	A_TP8
NFix	H	B2, B3	A1, B3	A1,A2	C3, A1
	L	B2, B1	B1, A1	A1=A2, A3	A1, C5
NLop	H	B2, D5	A1, B1	A1,C5	A1, C5
	L	B2, B1	B1, A1	A1,C5	C5, A1
		B_TP2	B_TP9	C_TP7	C_TP10
NFix	H	A1, B3=B4	C2, B2	A1, D5	B1, C1
	L	A1, B3	C2, B2	D5, A1	B1, A1
NLop	H	A1, B3	C2, B2	D5, A1	B1, A1
	L	A1, D4	C2, B2	D5, A1	B1, A1

Of particular interest about these segments is the contribution of the large number of loops to *NFix*, since loops are part of *NFix* by definition. To examine this issue, we focused on the ratio *NLop*/*NFix* of the primary segments with respect to *NFix*. As listed in Table 7, the ratio varied from 30.0 (B2 of A_TP1H) to 66.3% (A1 of A_TP6H) in Group H, and from 30.2 (A2 of A_TP6L) to 67.4% (A2 of A_TP6L) in Group L. Out of 17 ratios, 12 were greater than 50.0%. Four of them were the maximum values of the respective distributions: 66.3 (A1 of A_TP6H), 67.4 (A1 of A_TP6L), 55.6 (C2 of B_TP9), and 55.6 (B1 of C_TP10).

Table 7. NLop/NFix ratio of the first modal segments

	A_TP1	A_TP3	A_TP6	A_TP8
H	B2: 30.0	A1: 63.8	A1: 66.3	C3: 34.0
L	B2: 52.2	B1: 59.2	A1: 67.4, A2: 30.2	A1: 57.8

	B_TP2	B_TP9	C_TP7	C_TP10
H	A1: 46.0	C2: 45.0	A1: 55.6	B1: 57.1
L	A1: 52.0	C2: 55.6	D5: 60.4	B1: 55.6

Even the small ratios (30.0 and 34.0) less than 40.0 in Group H were the median of the distributions within the respective TPs.

B. Network analysis

1) Basic properties

Networks were constructed from the adjacency matrices, after removing the loops, for the individual TPs and Groups H and L. In all networks, 25 segments participated as nodes, being linked to other segments except for the isolated node E5 of A_TP3H.

As listed in Tables 8 and 9, the networks of Group H tended to have greater number of two-way and one-way links than those of Group L. An exception was found in the number of two-way links for A_TP6 (87 vs. 88 for H and L, respectively) and one-way links for C_TP7 (129 vs. 138).

The group difference in the number of two-way links was relatively constant, ranging from 24 to 36 in absolute values, except for A_TP6 (1) and C_TP10 (17). In contrast, the group difference in the number of one-way links varied more widely between 9 (C_TP7) to 42 (A_TP1) in absolute values. The variances were 115.9 and 203.8 for two-way and one-way links, respectively.

Table 8. Basic network properties for Type A

	A_TP1		A_TP3		A_TP6		A_TP8	
Index	H	L	H	L	H	L	H	L
Number of links								
two-way	112	82	92	68	87	88	102	77
one-way	171	129	122	116	143	121	156	129
total N^a	395	293	306	252	317	297	360	283
Reciprocity	.396	.389	.430	.370	.378	.421	.395	.374
Transitivity	.558	.488	.520	.472	.505	.468	.541	.435

Note[a]: A two-way link consists of two links in opposite directions, i.e., $N_{total} = 2 \times N_{two-way} + N_{one-way}$.

Table 9. Basic network properties for Types B and C

	B_TP2		B_TP9		C_TP7		C_TP10	
Index	H	L	H	L	H	L	H	L
Number of links								
two-way	102	72	114	84	101	65	78	61
one-way	161	150	141	132	129	138	202	186
total N^a	365	294	369	300	331	268	358	308
Reciprocity	.388	.324	.447	.389	.439	.320	.279	.247
Transitivity	.552	.457	.492	.462	.465	.448	.493	.443

Note[a]: A two-way link consists of two links in opposite directions, i.e., $N_{total} = 2 \times N_{two-way} + N_{one-way}$.

Reciprocity is an index, defined as the ratio of the number of two-way links to the total number of links, is not sensitive to the group size, namely the number of the fixation records. Since the index was less than .500 in all cases, the two-way links were not dominant. Even so, it was consistently greater for Group H than Group L with an exception of A_TP6 (.396 vs. .421).

Similar tendency was observed in *transitivity*, defined as

the probability that the adjacent nodes of a node are also connected, which was consistently greater for Group H than L with the difference lying between .017 (C_TP7) and .106 (A_TP8).

2) Core-peripheral Nodes

The nodes that were ranked highest at least in three indices were identified as the core (or peripheral). Shown in Tables 10 and 11 are the core nodes for each TP and Group. Two networks of Group L lacked cores: A_TP1L and C_TP7L. Instead, the network for A_TP3L contained dual cores, A1 and A3. Among the cores, A1 was predominant across pages and groups. The two exceptions were A2 of C_TP10H and A3 of A_TP3L.

Table 10. Ranks of the core nodes of the networks of Group H by index and TP

	A_TP1H	A_TP3H	A_TP6H	A_TP8H
Index	A1	A1	A1	A1
Degree	1	1	1	1
Closeness	1	12	16	1
Betweenness	1	6	14	1
PageRank	1	1	1	1
Authority-score	1	2	1	2
Hub-score	2	1	2	1

Table 10 (Cont'd). Ranks of the core nodes of the networks of Group H by index and TP

	B_TP2H	B_TP9H	C_TP7H	C_TP10H
Index	A1	A1	A1	A2
Degree	1	1	1	2
Closeness	2	2	8	1
Betweenness	1	3	12	1
PageRank	1	1	1	1
Authority-score	3	1	1	2
Hub-score	1	2	2	2

Concerning the peripheral nodes that were ranked least at least in three indices, E5 was the peripheral in all the networks except for those of C_TP7H and C_TP7L where none of the nodes met the criterion. Three networks had additional, or dual, peripherals: E3 of A_TP3L, E4 of B_TP2, and E4 of C_TP10. It is noteworthy that all the cores were located in the top row A, while the peripherals were located in the bottom row E.

Table 11. Ranks of the core nodes of the networks of Group L by index and TP

	A_TP1L	A_TP3L		A_TP6L	A_TP8L
Index	none	A1	A3	A1	A3
Degree	n.a.	1	2	1	3
Closeness	n.a.	4	1	13	1
Betweenness	n.a.	3	1	5	1
PageRank	n.a.	3	1	1	1
Authority-score	n.a.	1	10	1	8
Hub-score	n.a.	1	8	1	9

	B_TP2L	B_TP9L	C_TP7L	C_TP10L
Index	A1	A1	none	A1
Degree	1	1	n.a.	1

Closeness	2	3	n.a.	3
Betweenness	1	5	n.a.	8
PageRank	3	1	n.a.	1
Authority-score	6	1	n.a.	4
Hub-score	1	1	n.a.	1

3) Core neighborhood

The neighborhood of a given core is a subgraph consisting of the core and its directly linked nodes. When there were more than one cores in a network, their neighborhoods were combined by their union ($\cup$).

Table 12. Size of the core-neighborhood by TP and Group, with the *Jaccard* index

	A_TP1	A_TP3	A_TP6	A_TP8
Group				
H	10 (3, 5)	12 (4, 5)	10 (3, 4)	11 (3, 3)
L	n.a.	14 (5, 5)	8 (3, 2)	7 (5, 1)
Jaccard	n.a.	.529	.636	.286
	B_TP2	B_TP9	C_TP7	C_TP10
Group				
H	16 (5, 4)	11 (4, 3)	13 (5, 4)	9 (5, 3)
L	10 (4, 3)	10 (3, 3)	n.a.	11 (5, 2)
Jaccard	.444	.750	n.a.	.538

Note: The numbers of member nodes in rows A and B are put in parentheses. n.a. means the lack of cores.

The groups were similar in the median of the neighborhood size (11 and 10 for Groups H and L, respectively) and the range of the size, i.e., 7. However, they slightly differed in the minimum and maximum values of the size (see Table 12): [9 (C_TP10H), 16 (B_TP2)] for Group H, and [7 (A_TP8L) to 14 (A_TP3L)] for Group L. The group difference in size lay between one (B_TP9) to six (B_TP2).

Common to both groups, the majority of the neighborhood members belonged to rows A or B of the mesh, ranging from 6 out of 11 (A_TP8H) to 8 out of 9 (C_TP10H) in Group H, and 6 out of 10 (B_TP9L) to 6 out of 7 (A_TP8L). This motivated us to compute the *Jaccard* index to measure the neighborhood similarity between the groups (see Appendix), where applicable.

The similarity was quite low (.286) for A_TP8, mostly due to four members in row C and one in E for Group H that were not included in the neighborhood of Group L. The value of the index was moderate (.444$\leq J \leq$.538) on three TP's (A_TP3, B_TP2, and C_TP10) and high (.636$\leq J \leq$ .750) on two TP's (A_TP6 and B_TP9).

The spatial distribution of the neighborhoods will be displayed later in the joint analysis.

4) Clique-based communities

The size of the largest cliques was approximately the same across TP's and groups, varying between 5 and 7. However, the number of such cliques differed greatly, varying between 1 and 11 in Group H, and 1 and 15 in Group L.

The communities were constructed by union of the largest cliques for each TP and group. In the cases with a single largest clique, union was taken with a null set. The size of the largest cliques was 6 or 7 in Group H, and 5 or 6 in Group L.

Shown in Table 13 are the size of the communities with the parenthesized number of constituent nodes belonging to rows

A and B. Also shown are the *Jaccard* indicies that measured the community similarities between the groups.

Table 13. Size of the communities by Group and TP, associated with the *Jaccard* index

	A_TP1	A_TP3	A_TP6	A_TP8
Group				
H	13 (5, 5)	7 (4, 3)	10 (3, 4)	15 (3, 4)
L	7 (4, 3)	17 (4, 5)	18 (4, 4)	5 (2, 3)
Jaccard	.538	.412	.400	.333
	B_TP2	B_TP9	C_TP7	C_TP10
Group				
H	8 (4, 3)	7 (4, 3)	12 (3, 2)	16 (4, 5)
L	16 (5, 2)	6 (4, 2)	11 (5, 4)	9 (5, 4)
Jaccard	.412	.857	.438	.471

Note: The numbers of member nodes in layers A and B are put in parentheses.

The groups were similar in median of the community size (11 and 10 for Groups H and L, respectively), but differed in range: 7 (A_TP3H and B_TP9H) to 16 (C_TP10H) for Group H, and 5 (A_TP8L) to 18 (A_TP6) for Group L. Within each TP, the group difference was smallest (one) on B_TP9 and C_TP7, and largest (10) on A_TP3 and A_TP8.

The smallest group difference led to the greatest similarity in the *Jaccard* coefficient (.857) only in the case of B_TP9. The value was much smaller (.438) for C_TP7.859, probably owing to the low concentration of the members in rows A and B (five out of 12).

The largest group difference led to the smallest similarity (.333) only for A_TP8. The similarity was moderate (.412) for A_TP3. In the remaining cases, the similarity was moderate (.400$\leq J \leq$ .538).

5) Overlaps between communities and neighborhood

The cliqued-based communities and core neighborhoods will be referred to simply as communities and neighborhoods hereinafter.

An overlap in the set terminology refers to the intersection of two sets under study. Hence, in the present context, the members in the intersection of a community and a neighborhood belong to both subgraphs. The degree of overlap, or the coincidence of the membership, was measured by the *Jaccard* index and shown in Table 14.

Table 14. Coincidence of member nodes in the communities and the neighborhoods

Group	A_TP1	A_TP3	A_TP6	A_TP8
H	.643*	.583*	.818*	.625*
L	n.a.	.722*	.300	.333
Group	B_TP2	B_TP9	C_TP7	C_TP10
H	.500*	.636*	.316	.471*
L	.529*	.600*	n.a.	.538*

Note: * indicates that the community contained the respective core(s).

The coincidence was low ($\leq$ .333) in the cases where the communities did not contain the cores: C_TP7, A_TP6L, and A_TP8. Moderate coincidence (.471$\leq J \leq$.583) was found on A_TP3H, B_TP2H and C_TP10H. The rest were high (600$\leq J \leq$.722) and very high (.818); A_TP1H, A_TP8H, B_TP9H, B_TP9L, and A_TP6H.

More limited concern is the membership of the cores in the communities. All of the communities with moderate or higher coincidence ($\leq$.471) included the respective cores, even when there were two cores (A_TP3L).

C. Joint analysis of heat maps and subgraphs

To aid joint analysis, the heat maps were overlaid with the corresponding communities, and then with the neighborhoods as shown in Figures 5 through 8. In these figures, the links connected to (inward) and from (outward) the cores within the individual communities are specially colored.

Table 15. Heat grade of the cores by Group and TP

Group	A_TP 1	A_TP3	A_TP 6	A_TP8
H	A1*: 3	A1*: 1	A1*: 1	A1*: 2
L	n.a.	A1*: 2, A3*: 4	A1: 1	A3: 4
Group	B_TP2	B_TP9	C_TP7	C_TP1 0
H	A1*: 1	A1*: 4	A1: 1	A2*: 4
L	A1*: 1	A1*: 4	n.a.	A1*: 2

Note: * indicates that the cores belong to the respective communities.

If the core node is included in the community and it also belongs to the heated segment (say, grade 3 or above), we can say that the correspondence between relational and cumulative importance is fairly good. If most of the neighborhood members also belong to the heated segments, say grade 3 or higher, the correspondence increases further.

First, among 10 cases in which the cores are included in the communities (see Table 15), the cores, (A1), of A_TP3H, A_TP6H, B_TP2H and B_TP2L belonged to the most heated segments, i.e., grade 1. In the other cases, the cores, (A1), of A_TP8H, A_TP3L, and C_TP10L were less heated (at grade 2), followed by A1 of A_TP1H whose heat grade was three. The grade of the dual core A3 of A_TP3L was four.

Second, two of the three cores lying outside of the respective communities were the most heated segments (grade 1): A1 of A_TP6L and C_TP7H. A3 of A_Tp8L was at grade 4.

When the scope of inspection was broadened to the neighborhood level, the heat of the neighborhood members were widely distributed mostly within the range of [1, 5]. The lowest heat grade (six) was found in two neighborhoods in Group H, and one in Group L: A_TP8H (E2), B_TP2H (A3, B3 and E2), and A_TP2L (A4).

Figure 5. Heat map overlaid with the communities (with large dark nodes) and the neighborhoods (with small light nodes) of TPs 1 and 3 of Type A by Group
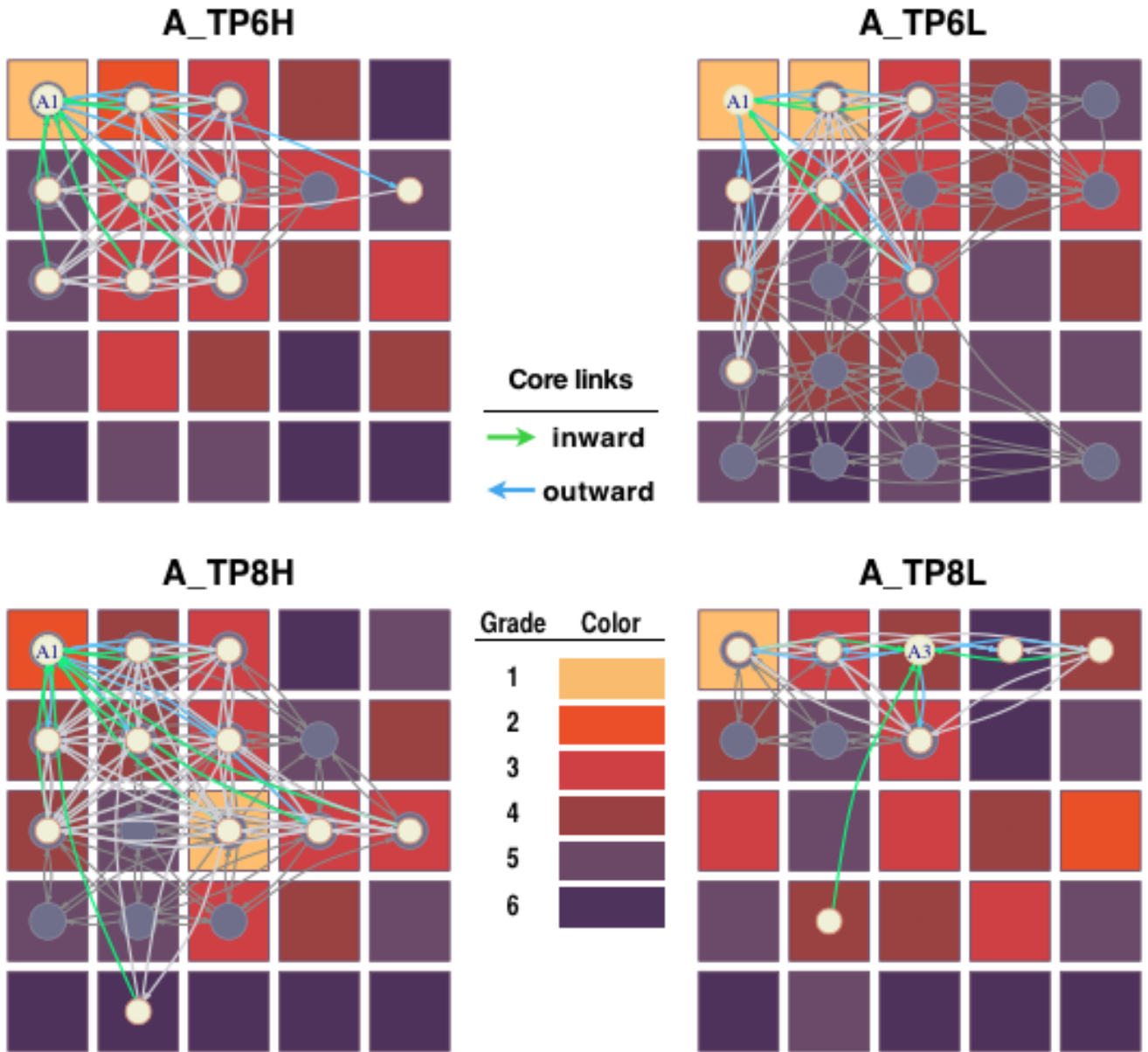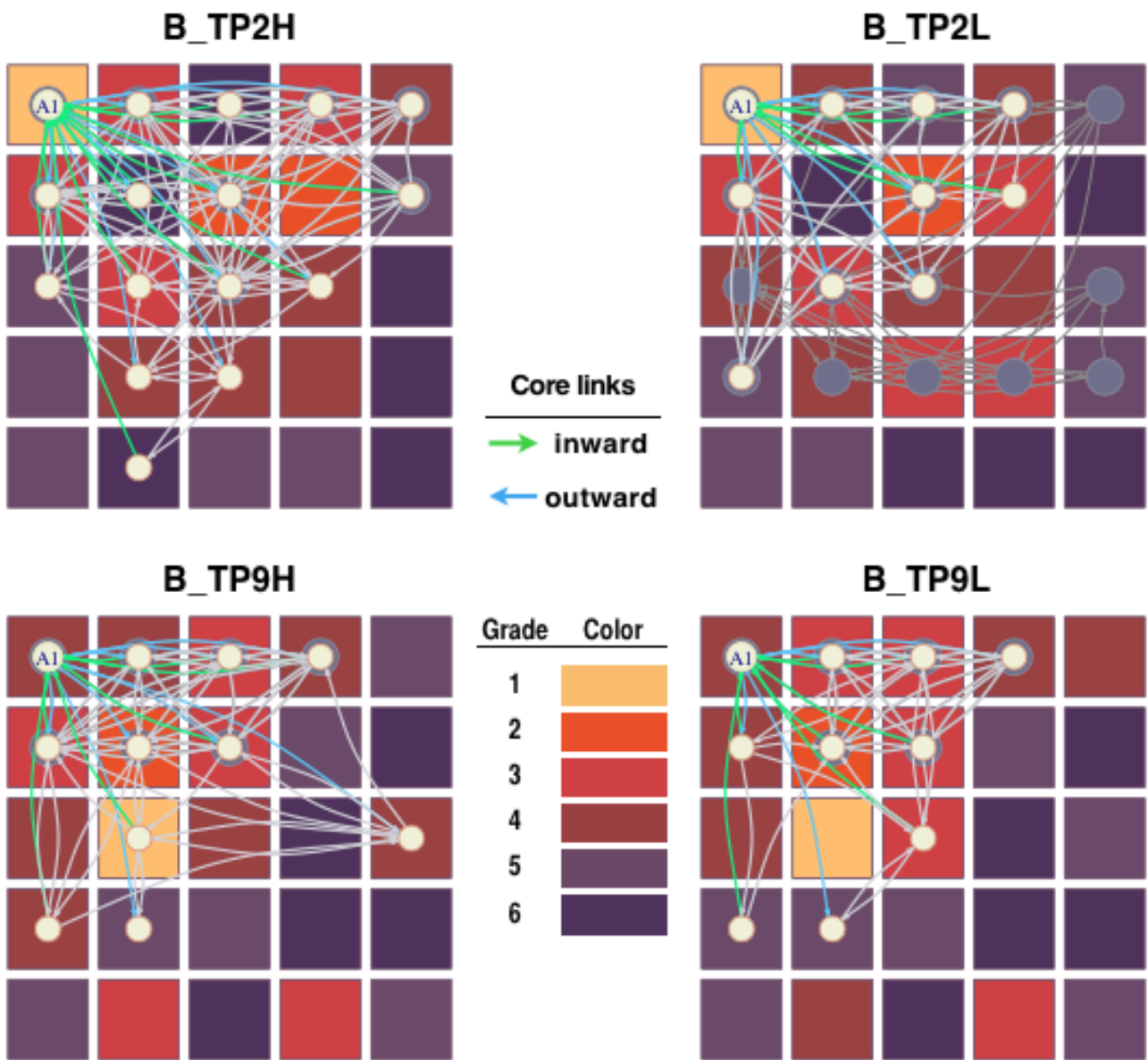[Note] The core nodes are marked with labels.
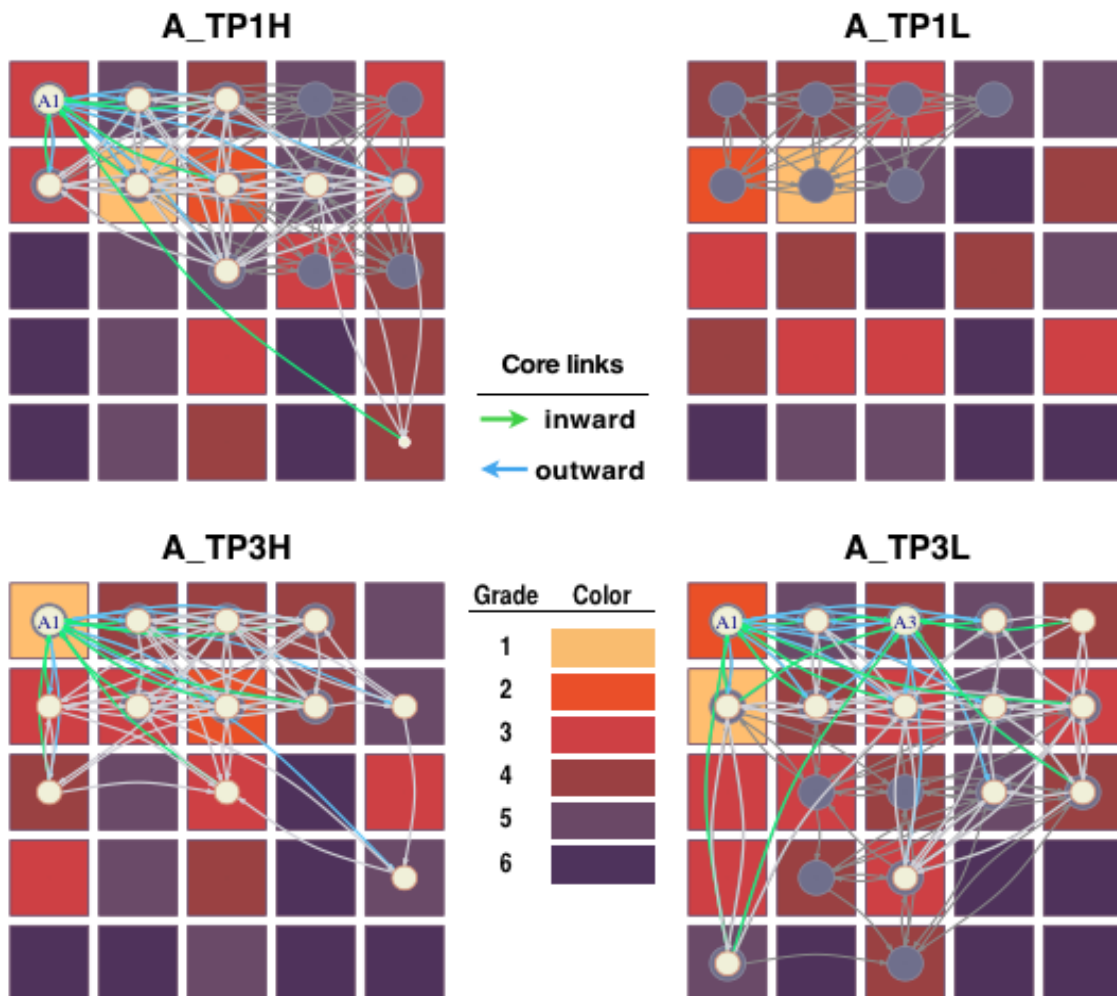
Figure 6. Heat map overlaid with the communities (with large dark nodes) and the neighborhoods (with small light nodes) of TPs 6 and 8 of Type A by Group
[Note] The core nodes are marked with labels.

Figure 7. Heat map overlaid with the communities (with large dark nodes) and the neighborhoods (with small light nodes) of TPs 2 and 9 of Type B by Group
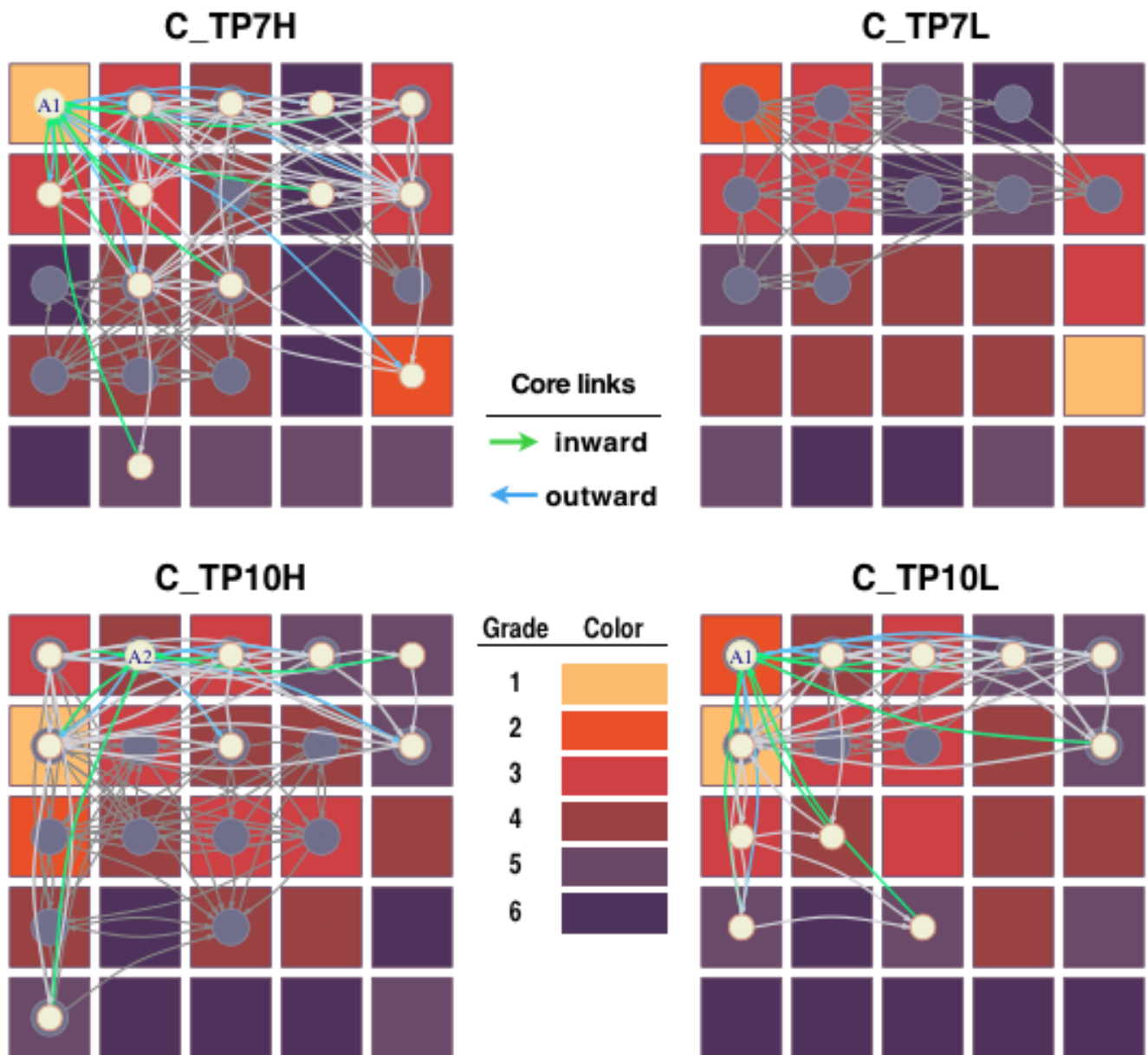[Note] The core nodes are marked with labels.

Figure 8. Heat map overlaid with the communities (with large dark nodes) and
the neighborhoods (with small light nodes) of TPs 7 and 10 of Type C by Group
[Note] The core nodes are marked with labels.

IV. Discussion

The purpose of the present work was to compare the heavy and light user groups with respect to the cumulative importance in the number of fixations (*NFix*) and the number of loops (*NLops*), in addition to the relational importance in the various network properties.

Concerning the cumulative importance, the two user groups appeared to be quite similar both in *NFix* and *NLop* across TPs in the *Pearson*'s product-moment correlation coefficient. However, the similarity decreased in varying degree across TPs in the *Kendall*'s rank-order correlation coefficient. Although the evidence seems to imply some regularity about the group difference, inspections of the median and the mean showed puzzling, incongruent patterns of *NFix* and *NLop*.

The best we can point is that the metric (the *Pearson*'s coefficient and the mean) and nonmetric (the *Kendall*'s coefficient and the median) measures shed light on the data from different perspectives. For instance, the metric measures are sensitive to a few extreme values, the latter remain unaffected by them. To the extent the results agree, we gain confidence. If they disagree or are inconsistent, we should refrain from drawing hastily conclusions about the extent of similarities. We are planning to inspect our data more closely in this regard.

Introductory statistics textbooks teach us that the mean, median and mode are the measures of the central tendencies of a given distribution. And, it is the modal segments of *NFix* and *NLop* in which the groups agreed fairly well across pages.

These segments bear primary static (cumulative) importance. The question that immediately arises is whether the location of static and dynamic importance agreed or not.

As reported in Results, perfect agreement was found in four networks whose cores, all belonging to the respective communities, were the most heated segments, i.e., heat grade 1. At grade 2 (and 3), three (and 1) network(s) showed the similar agreement.

Being the community member was not a sufficient condition for the good agreement between the core status as evidence by the low heat (grade 4) of the cores in the networks for Groups H and L on the same TP (B_TP9). Neither was it a necessary condition, as evidenced by the nearly agreement of the dynamic and static importance in two networks, one for Group H and the other for Group L. The cores of these networks were not contained in the communities, but the segments were most heated (i.e., grade 1).

As to the group difference in joint analysis of the importance, the presence of the dual cores and the absence of cores were observed in Group L alone. Other than this, the groups were mostly similar with minor differences.

When the scope of analysis was moved from individual nodes to groups of nodes, interesting group differences emerged. That is, Group H had higher levels of *reciprocity* and *transitivity* than Group L across pages with a single exception in *reciprocity*. In a word, shifts of attention of Group H were more often reciprocated between nodes and more tightly related in the triangular form, as compared to Group L.

Nevertheless, these close relationships were too local to influence the formation of clique-based communities. Note that the *reciprocity* applies to pairs of nodes, and the *transitivity* applies to triads of nodes. The spans of nodes covered by these indices are too small in view of the size of the largest cliques that ranged from 5 to 7. Besides, two-way links are treated as undirected one-way links in the clique identification. Therefore, it is not surprising to find that the groups differ in the community size in the complex manner.

As a whole, there was no clear-cut group difference. They were similar in some respect, and differed in others. Perhaps there is no factor that will thoroughly differentiate users. Still, we should continue our effort in hope of providing practical findings which could assist web designers for better communication with viewers.

V. Appendix: The *Jaccard* index

The *Jaccard* index is a similarity coefficient between two sets of elements. It is defined as the ratio of the size of the union ($\cup$) to that of the intersection ($\cap$). The following examples illustrate the point in the context of the present study:

Set H: {A1, A2, B2, C3}
Set L: {A1, B2, C4, D5, E2}
the union: {A1, A2, B2, C3, C4, D5, E2}
the intersection: {A1, B2}

Hence, the value of the index for the two sets is 2/7. If the sets share all (or none) of the elements, the value is one (or zero).

References

[1] S. Brin, L. Page, L. "The anatomy of a large-scale hypertextual web search engine", *Computer Networks and ISDN Systems*, *30*, pp. 107-117, 1998.

[2] G. Buscher, E. Cutrell, M.R. Morris. "What do you see when you're surfing? Using eye tracking to predict salient regions of web pages". In *Proceedings of CHI 2009*, pp. 21-30, 2009.

[3] G. Csardi, T. Nepusz. "The igraph software package for complex network research". *InterJournal, Complex Systems"*. 2006, http://igraph..net/

[4] L.C. Freeeman. "Centrality in social networks", *Social Networks*, 1, pp. 215-239, 1979.

[5] J.H. Goldberg, X.P. Kotval. "Computer interface evaluation using eye movements: Methods and constructs", *International Journal of Industrial Ergonomics*, *24*, 631-645, 1999.

[6] L.A. Granka, H.A. Hembrooke, G. Gay. "Location location location: Viewing patterns on WWW pages". In *Proceedings of Symposium on Eye Tracking Research & Applications* (*ETRA2006*), p.43, 2006.

[7] S. Josephson. "A Summary of eye-movement methodologies". *FactOne*, 2004. http://www.factone.com/article_2.html

[8] M. Kleinberg. "Authoritative sources in hyperlinked environment", *Journal of the ACM*, *46*(5), pp.604 -632, 1999.

[9] L. Lorigo, M. Haridasan, H. Brynjarsdottir, L. Xia, T. Joachims, G. Gay, L. Granka, F. Pellacini, B. Pan. "Eye tracking and online search: Lessons learned and challenges ahead", *Journal of the American Society for Information Science and Technology*, *59* (7), pp.1041-1052, 2008.

[10] N. Matsuda, H. Takeuchi. "Networks emerging from shifts of interest in eye-tracking records", *eMinds*, *2*(7), pp.3-16, 2011(a).

[11] N. Matsuda, H. Takeuchi. "Joint analysis of static and dynamic importance in the eye-tracking records of web page readers", *Journal of Eye Movement Research*, Vol.4(1):5, pp.1-12, 2011(b).

[12] M.E.J. Newman. "The structure and function of complex networks", *SIAM Review*, *45*(2), pp. 167-256, 2003.

[13] J. Nielsen, K. Pernice. *Eyetracking web usability*. Berkeley, CA: New Riders, 2010.

[14] B. Pan, H. Hembrooke, G. Gay, L. Granka, M.K. Feusner, J. Newman. "The determinants of web page viewing behavior: An eye-tracking study". In *Proceedings of Eye Tracking Research & Applications* (*ETRA2004*), pp.147-154, 2004.

[15] R Development Core Team. *R: A language and environment for statistical computing*. R Foundation for Statistical Computing, Vienna, Austria. ISBN 3-900051-07-0, http://www.R-project.org, 2008.

[16] S. Wasserman, K. Faust. *Social network analysis: Methods and applications*. Cambridge University Press: Cambridge, 1994.

Author Biographies

Noriyuki Matsuda has recently been engaged in the analysis of the information design and users' behavior, stemming from his deep concern with the intricate interplay between cognition and affect, called *kansei* in Japanese, blended with his background in Experimental Psychology (M.A. at Emory University, USA, 1975) and Sociology (Ph.D. at Univ. of Maryland, USA, 1980). He is now working as a professor at the Graduate School of Information and Systems Engineering of the University of Tsukuba, Japan. For more information, please visit my site at http://www.sk.tsukuba.ac.jp/~mazda.

Haruhiko Takeuchi was born in Kyoto, Japan in 1958. He received his master's degree in engineering from the University of Tsukuba in 1984. He is a senior research scientist in the Human Technology Research Institute at the National Institute of Advanced Industrial Science and Technology (AIST), Japan. His research interests include eye-tracking data analysis, data mining, latent semantic analysis, Fuzzy theory and neural networks.